Multiface Unity

© **L. I. Matveyenko**

Space Research Institute, Moscow, Russia

Our studies of the fine structure of active regions of star formation Orion KL, W3OH, and AGN objects: 3C 84, M 87, 1803+784, 3C345, 3C454.3 NGC 4258, Cyg A, that are corresponding to the vortex. Instability of progressive movement leads to a turbulence. The matter floats onto the disk, and transferred in a spiral arm to the center. Excess angular momentum in process of accumulation is caring away by a bipolar out flower. The Keplerian movement of peripheral part of a whirlwind turns into rigid body rotation. The rest of matter drops out on the formed massive body. The bipolar out flowers represent the rotating coaxial tubes. Interaction with surrounding matter collimates and accelerates streams. In plasma generated ring currents — magnetic fields. The jet is moving along the magnetic field — accelerating and the counter jet against — deaccelerating.

Keywords: VLBI, AGN, masers.

1 Introduction

The object structure contains main information about its nature and the processes proceeding in it. Especially it belongs to active compact regions of star formation regions and nuclei of galaxies. Ultrahigh angular resolutions are necessary for the solution of these problems. VLBI method opened this possibilities [1]. The fine 3D structures of star formation region of Orion KL, and W3OH in maser emission are corresponding to vortex. The same structure in maser emission have Galaxy and NGC 4956, and in continuum AGN objects 3C 84, 3C 345, 3C 454.3, 1803+784, M 87 NGC 4258 and Cyg A. The structures are corresponding to vortex over a sea surface. We will consider peculiarities of these objects.

2 Orion KL

The maser radiation of molecules of water vapor accompanying processes of stars formation that allowed define thin 3D structure of active region. The vortex structure had been opened in a dense molecular cloud of the Orion Nebula [2]. The structure representing a chain of compact sources distributed along the S-shaped component — disk $\phi = 28$ AU, observed from an edge. The surrounding matter

flows on a spiral trajectory to the center, tangential directions of which are corresponding to chain compact sources. The arising excess angular momentum is carrying away by a bipolar outflow, high-velocity central, surrounding by low-velocity one, Fig. 1. Diameter of the low-velocity nozzle is $\phi = 0.9$ mas, Fig. 1 (left). Velocity of ejected of matter exponential increases as approaching the center. Remain of medium drops out on the formed central body. As a result, the Keplerian movement of an outflow passes in rigid body rotation in the central part of a disk $\phi = 15$ A. U. The period rotation of disk is 170 years. Ejection velocity of the outflow $v \geq 5$ km/s, and is increasing until $v \geq 40$ km/s at distance 2 A. U., Fig. 2a. b. Interaction of the rotated outflow with environment medium is collimating and accelerating it [3]. Gas dynamic instability of the outflow causes the precession — spiral structure, and the jet reactive influence bends a disk, giving it the S-shaped form. The same structures are observing in hydroxyl maser emission at 1665 MHz in an object W3 OH. The rigid-bod rotation disk and bipolar outflow. We will consider objects with the same peculiarities [4].
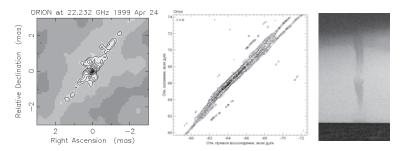

Fig. 1. Region of low and high velocity nozzles (*left*); high-velocity bipolar outflow, surrounded by low velocity component (*center*); Coaxial structure of jet Black sea (*right*)

3   Whirlwinds

Instability of progress movement of air streams over a sea surface leads to formation of whirlwinds. Water drops light structure and kinematics of a whirlwind. The air stream arrives to a whirlwind and flows on a spiral to the center. Rotation velocity of a stream increases exponential. Process of accumulation of excess angular momentum is accompanying by ejection of outflows, forming coaxial tubes, the surrounding the central high-speed stream. The height of tube is determining by speed, Fig. 1 (right). Interaction with surrounded medium collimates and accelerates the outflow. Now we will consider the main objects of Universe galaxies.

4   Galaxies structure in spectra- line emission

Our Galaxy in infrared radiation corresponds to whirlwind. Excess angular momentum is caring away by a bipolar out flow and Keplerian movement of gas medium is passing in rigid-body rotation in the central part. NGC4258 galaxy represents a
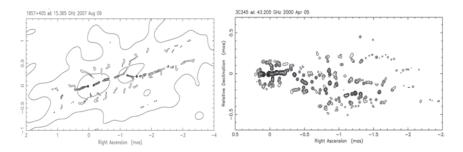
Fig. 2. Map of Cyg A, $\lambda = 2$ cm, $\phi = 20$ μas (*left*); 3C 345, $\lambda = 7$ mm, $\phi = 20$ μas (*right*)

two-arm spiral with a bar. Water vapor maser radiation allowed investigated 3D structure — distribution of cold gas. Keplerian movement in remote parts passes in rigid-body rotation of the central part. The maser radiation is concentrated in two peripheral and the main central group [5]. The central group is dividing into two parts, radiation of which exponentially increases as approaching the center, and determined by tangential directions of arms. A pumping of maser emission determined by an infrared radiation of the core. Absent of maser emission in the center causes by high temperature of a matter, synchrotron emission of which — bipolar out flower is visible in a continuum. The maser emission of the peripheral groups is determining by collisions pumping, acceleration of matter. The increased velocity of the hydrogen molecules relatively of water vapor is defined difference of masses. We will consider structures of galaxies in the synchrotron emission.

5   Galaxies structure — synchrotron emission

We are studied the fine structure of AGN objects of: 3C 273, 3C 345, 3C 454.4, Cyg A, 3C 84, M 87, 1803+784 in the synchrotron emission. In this case structure determined by distribution and kinematics of relativistic plasma. The fine structures determined by compact bright source nozzle, disk, and bipolar out flower. Brightness temperature of the nozzle $T_b \geq 1^{12} K$ and corresponds to emission of ejecting relativistic electrons. Ejection velocity are $v \leq 0.06 \ c$. Structure of counter jet is mirror reflection of jet. The bigger jet size is determining by acceleration. CygA counter sizes < 0.8 mas at $\lambda = 2$ cm, resolution to $\varphi = 20$ μas, but jet 3 mas, [6], Fig. 2. The brightness temperature of nozzle corresponds to $T_b = 4 \cdot 10^{12} K$. The central high-velocity bipolar outflow is located between parallel chains of compact components, the carried on 0.7 mas. The chains are corresponding to the tangential directions of walls of low-velocity tube. The rotation of the tube is generating currents, which contracting in rings solenoid, magnetic field of the outflow.

3C 273 quasar, the brightness temperature of the nozzle, $\lambda = 2$ cm, $\varphi = 20$ μas as $T_b \geq 140 \cdot 10^{12} K$. The high-velocity counter jet is visible until ≤ 3 pc. The jet is visible > 3 pc, but brightness of fragments is weaker than low-velocity components. It mean that main part of matter is ejecting by low-velocity nozzle. The ejection velocity is $v \leq 0.03 \ c$. 3C 345 Fig. 3c, $\lambda = 7$ mm, $\varphi = 20$ μas, structure
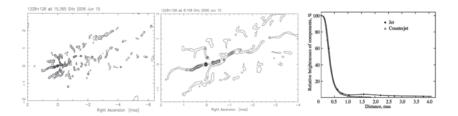
Fig. 3. M 87, $\lambda = 2$ cm (*left*), $\phi = 50\mu$as (*center*); $\lambda = 3$ cm; distribution brightness of bipolar outflow (*right*)

is similar: nozzle and high-velocity bipolar outflow is surrounding by low-velocity fragments [7]. Jet sizes exceed counter jet approximately by seven times, Fig. 2. The ejection velocity is $v \leq 0.06\ c$, and $v \simeq 8\ c$ at distance 0.5 pc. The bipolar out is clear expressed at $\lambda = 2$ cm. The brightness temperature of nozzle is $T_b = 50 \cdot 10^{12}$ K. The emission of ejected relativistic electrons is decreasing exponentially/ But jet has long tail post emission of the electrons similarly M 87, Fig. 3.

M 87 structure at $\lambda = 2$ cm, $\varphi = 0.1$ mas is typical for AGN objects: nozzle, high-velocity bipolar out flower, surrounding by low-velocity it, Fig. 3. The high-velocity jet is much bigger that counter jet. An acceleration is compensating radiation loses of the jet. Structure of low-velocity counter-jet is horn-form at $\lambda = 3$ cm. Diameter of the tube is increasing of $\phi = 1.0$ mas to of $\phi = 2$ mas in remote part that propose decreasing of nozzle. The jet structure is similar, but smooths by big length more than 4 times [8].

1803+784 disks is parallel to sky plane $\lambda = 18$ cm $\varphi = 100\ \mu$as, Fig. 4. Circular structures correspond to nozzle of low-velocity out-flow, $\phi = 2.7$ mas. The central high-velocity counter-jet is much smaller than jet. The nozzle brightness temperature $T_b = 20 \cdot 10^{12}$ K. At $\lambda = 3$ cm, as well as earlier, is observed the ring structure corresponding to a nozzle of a low-velocity outflow, $\phi = 1$ mas, Fig. 4. The brightness of a counter jet nozzle is $T_b = 12 \cdot 10^{12}$ K. The jet is ejecting in the opposite direction and seen from distance of 0.4 mas outside of absorbing part of a disk. The jet is surrounding by a low-velocity tube. Diameter of the low-velocity nozzle is equal 0.23 mas, $\lambda = 7$ mm.
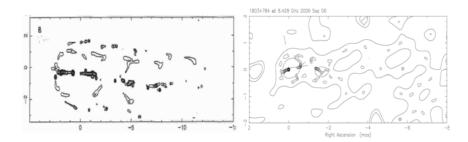

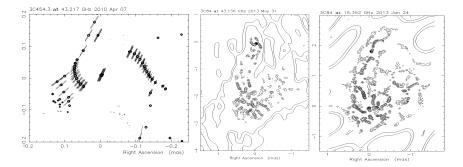Fig. 4. 1803+784, $\lambda = 18$ cm, $\phi = 0.1$ mas (*left*); $\lambda = 3$ cm, $\phi = 50\mu$as (*right*)

Fig. 5. 454.3, $\lambda = 7$ mm, $\phi = 2.5$ μas (*left*); 3C 84 $\lambda = 7$ mm, $\phi = 25$ μas (*center*); $\lambda = 2$ cm (*right*)

3C 454.3 structure consists of a disk orients in the sky plane, and jet with the bent axis, surrounding by low-velocity tube, $\lambda = 2$ cm. The ejector brightness temperature is $T_b = 4 \cdot 10^{12}$ K. The fragments of arms, of which are ejecting matter caring away extra angular momentum, are observing $\lambda = 7$ mm, resolution 2.5 μas, Fig. 5. The brightness nozzle temperature $T_b = 200 \cdot 10^{12}$ K [9]. NGC 1275 galaxies, are connecting gravitationally. Differential velocity is 600 km/s, that corresponds to orbital period $T = 10^3$ years, and mass of the black holes $M = 10^7 M\odot$. The high-velocity bipolar out flows of the systems are surrounded by low-velocity tubes. The diameter eastern tube is $\phi = 0.6$ mas, and western $\phi = 1.5$ mas, $\lambda = 2$ cm, and $\lambda = 7$ mm, Fig. 5. The brightness temperature of the nozzles $T_b = 4 \cdot 10^{12}$ K [10].

6 Conclusion

Superfine structure of star formation regions and AGN objects corresponds to whirlwind. Instability of progress of gas leads to a turbulence and running off on a spiral arm to the center. Excess angular momentum is caring away in process of its accumulation by the bipolar out flower coaxial tubes. The rest of medium drops out on the central body, gravitational field of which accelerates and stabilizes process. Interaction rotated streams with surrounding medium determinate collimation and acceleration. The ring currents magnetic fields are generating in plasma of a disk and out flowers. A jet and a counterjet is moving along and opposite a magnetic field that accelerates or brakes its.

The studies are supported by Program P21/2 of the Presidium RAN.

References

1. *Matveyenko L. I.* Early VLBI in the USSR. // Astron. Nachr. — 2007. — AN 328, N 5. — P. 411–419.

2. *Matveyenko L. I., Zakharin K. M., Diamond P. J., Graham D. A.* Evolution of the structure of the H2O super maser outburst regon in Orion KL // Astronomy Letters. — 2004. — Vol. 30, N 2. — P. 100–116.

3. *Abramyan M. G., Matveenko L. I.* Initial phase of protostar formation // Astrophysica — 2012. — Vol. 55, N 3. — P. 397–410.

4. *Matveenko L. I., Ipatov A. V., Demichev V. A., Melnikov A. E.* Structure of the Object W3 OH in Hydroxyl Maser Lines // Astronomy Letters. — 2014. — Vol. 40, N 2. — P. 95–110.

5. *Greenhill L. J., Jiang D. R., Moran J. M., et al.* Detection of a Super parsec Diameter Disk in the Nucleus of NGC 4258 // Astroph. J. — 1995. — Vol. 440. — P. 619.

6. *Matveyenko L. I., Seleznev S. V.* Fine Structure of the Jet from Cygnus A // Astronomy Letters. — 2015. — Vol. 41, N 12. — P. 743–747.

7. *Matveyenko L. I., Sivakon S. S.* Kinematics of the Active Region of the Quasar 3C 345 // Astronomy Letters. — 2013. — Vol. 39, N 8. — P. 481–512.

8. *Matveyenko L. I., Seleznev S. V.* Kinematics of the Nucleus of the Radio Galaxy M 87 // Astronomy Letters. — 2015. — Vol. 41, N 12. — P. 712–742.

9. *Matveyenko L. I., Sivakon S. S.* Active Region of the Nucleus of the Blazar 3C 454.3 // Astronomy Letters. — 2016. — Vol. 42, N 10. — P. 639–651.

10. *Matveyenko L. I., Seleznev S. V.* Fine Structure of the Nucleus of the Galaxy NGC 1275 // Astronomy Letters. — 2016. — Vol. 42, N 4. — P. 207–214.